

Investigation of non-local heat transport and its interplay with neoclassical tearing modes (NTMs) in the HL-2A tokamak

Y. Xu¹, X. Q. Ji¹, O. Pan¹, Yi Liu¹, W. L. Zhong¹, Z. B. Shi¹, M. Jiang¹, B. B. Feng¹, D. L. Yu¹, Y. Zhou¹, J. Cheng¹, M. Xu¹, W. Chen¹, Yuan Xu¹, Y. B. Dong¹, L. W. Yan¹, X. T. Ding¹, Q. W. Yang¹, X. R. Duan¹, Yong Liu¹ and the HL-2A team

¹ Southwestern Institute of Physics, P. O. Box 432, Chengdu 610041, People's Republic of China

C. Hidalgo²

² Laboratorio Nacional de Fusión, CIEMAT, 28040 Madrid, Spain

In fusion plasmas, a number of experiments for the study of transient transport events have revealed a striking phenomenon, i. e., a fast “non-local” response of the core temperature rising to an edge cooling executed at the plasma periphery [1-6]. A few common features are observed during this non-local transport (NLT): (i) the core electron temperature (T_e) quickly increases before the edge cooling pulse diffuses in; (ii) the NLT usually happens below a critical density or collisionality; (iii) the reversal radius of the opposite T_e variation on two sides is often located in the region of $1 < q < 2$. This transient and non-diffusive response with reversed polarity calls seriously into question of the standard “local” transport model, and hence, has puzzled scientists for more than twenty years. For understanding the physical processes of the NLT, various theoretical models have been proposed to explain the provocative non-local effects [3]. Among them the self-organized criticality (SOC) paradigm attempts to unravel the transport enigma via the interrelation between individual turbulent eddies and large-scale transport events like the “sand-pile” avalanche [7-10].

In this paper, we present the experimental investigation on the properties of SOC dynamics during the NLT at the HL-2A tokamak. The experiments were carried out in ohmically or ECRH heated plasmas. Typical discharge parameters were $R=1.65$ m, $a=0.38-0.40$ m, $B_T=1.3-1.45$ T, $I_p=150-165$ kA, $P_{ECRH}=1.2-2.0$ MW and $\bar{n}_e = (0.8-2.0) \times 10^{19}$ m⁻³. The non-local effects were induced in low density discharges by employing a SMBI system which made cold pulses at the plasma boundary [4]. For measuring the equilibrium and fluctuating T_e , a 16 channel ECE diagnostic was used and digitized at a sampling rate of 1.25 MHz. The Doppler reflectometer and Langmuir probes detected edge turbulence and poloidal plasma rotations, and Mirnov coils measured magnetic fluctuations.

Figure 1 plots discharge waveforms and multi-channel ECE signals in a typical NLT shot. Figure 1(a) shows that the I_p is constant and the SMB was injected at $t=1084$ ms during the stationary phase of the discharge. After the SMBI, the \bar{n}_e slightly increases due to fueling effects. Figure 1(b) displays the evolution of T_e at different radii. At the outer region, the SMBI cooled the plasma and caused reduction of T_e . However, in the core area the red curves show, surprisingly, increases in T_e . The reverse position, $r/a=0.47$, is around $q=3/2$ surface. It has been found that the density and temperature fluctuation levels are nearly unchanged before and during the NLT [11], implying that the turbulent transport is not directly contributive to the core

T_e rising via confinement improvement.

To investigate the role of SOC in the non-local transport, we have analyzed the Hurst parameter (H) in temperature fluctuations (\tilde{T}_e) before and during the NLT. The H is calculated by structure function (SF) [12] and R/S [13] methods in \tilde{T}_e data. Figure 2(a) shows an increase of H (with NLT) from 0.78 to 0.85 at $r/a=0.77$. The radial profile of Hurst exponents further indicates that the H values are generally enhanced in all radii in the nonlocal phase (see Fig. 2(b)). Besides, the cross-correlation function (CCF) of \tilde{T}_e between ECE channels has also been computed. The results show an increase of the radial correlation length in the propagation of avalanche events and stronger inward transport during the NLT [11]. These results explicitly point out an enhancement of SOC paradigm during the non-local period. This enhanced SOC behavior with NLT might be related to the reduced flow shear in the plasma edge, which is caused by increased damping (or cooling effects) of SMBI, as depicted in Fig. 2(c).

In this study, during the NLT at HL-2A, an intimate interaction between the neoclassical tearing modes (NTMs) and the nonlocality has been observed in ERCH heated plasmas [6]. As shown in Figs. 3(a) and (b), after injection of SMB at 838 ms the NLT is induced, and then an NTM is excited at $t\approx 844$ ms. The mode numbers

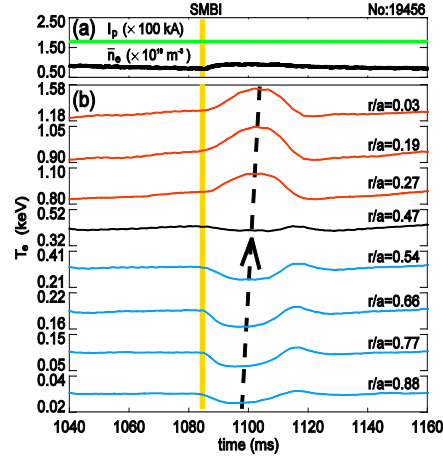


FIG. 1: Typical discharge waveforms of non-local transport induced by SMBI (vertical yellow bar) at HL-2A. (a) Plasma current and line-averaged density; (b) Multi-channel ECE signals showing decrease of T_e in the plasma edge (blue) and increase of T_e in the core (red).

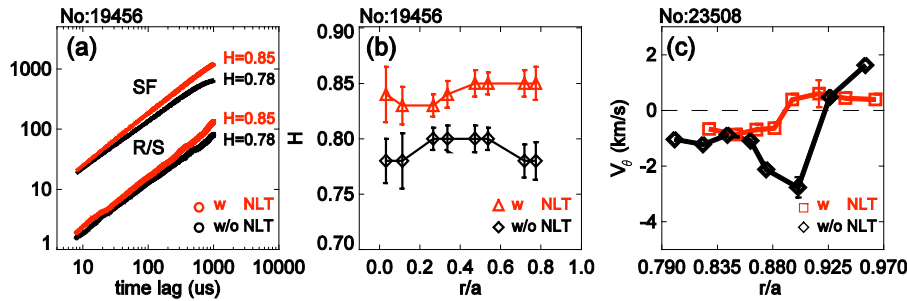


FIG. 2: Comparison of SOC features without NLT (black) and with NLT (red). (a) Hurst exponents calculated by SF and R/S methods at $r/a=0.77$; (b) radial dependence of Hurst parameters and (c) radial profile of the poloidal flow at plasma boundary.

have been identified as $m/n=3/2$ and frequency $f\approx 7$ kHz, as shown in the frequency spectrum of the SXR signal in Fig. 3(c). The neoclassical nature of the tearing modes is illustrated in Fig. 3(d), where the variation in the fluctuation amplitude of the radial magnetic field (square root of $\tilde{B}_r \propto$ island width) around the mode frequency ($f=6-9$

kHz) exhibits approximately a linear relation with β_N in five shots having the 3/2 islands. It is found that the reversion surface of the NLT is usually located at $q=3/2$ or 2/1 surface. Nearby the reversion surface, the increase of local temperature (or pressure) gradient results in increase of bootstrap currents, and hence, onset of NTMs at $q=3/2$ or 2/1 surface. As shown in Fig 3, no seeding island was seen prior to NTM onset, implying that the local pressure gradient grows strong enough to linearly drive the NTMs. Because of the non-local effect, the NTM can be triggered at lower β_N [14].

In the present study, significant influence of NTMs on the magnitude of nonlocal responses has been observed. Plotted in Figs. 4(a)-(e) are time evolutions of plasma density, multi-channel ECE signals and contour-plot of frequency spectrum of the SXR signal in a discharge with two nonlocal transport induced by edge gas-puffing. After the first gas-puffing at $t=570$ ms, the nonlocal effect appears and then the 3/2 NTM is excited with $f=6-8$ kHz, similar to that depicted in figure 3. After the NTM occurrence, the second gas-puffing is injected at $t=770$ ms, which also triggers a nonlocal transport. However, for the second nonlocality the changes of T_e in both edge and core regions are much smaller than the first one. To understand this phenomenon, we calculated the Hurst exponents and CCF in \tilde{T}_e during the first (without NTM) and second (with NTM) nonlocal periods. With NTM, the H values drop abruptly in the inner region, whereas in the outer area they are nearly unvaried (see Fig. 4(f)). The reduction of avalanche-like transport by the NTM can be more clearly seen in Figs. 4(g) and (h), where the contour-plot of CCF between ECE signals in the first and second NLT period are plotted. The figures show that with NTM the radial correlation in \tilde{T}_e remains large in the outer zone ($\rho \approx 0.6-0.8$), consistent with high Hurst parameters shown in Fig. 4(f). However, in the inner region ($\rho < 0.6$), the radial correlation of turbulent events is broken by the NTM. In HL-2A, we have measured the toroidal plasma rotation with the presence of a magnetic island [14] and found that the local flow shear inside the island is strongly enhanced when the island is wide enough, similar to that observed in LHD [15]. According to theories and

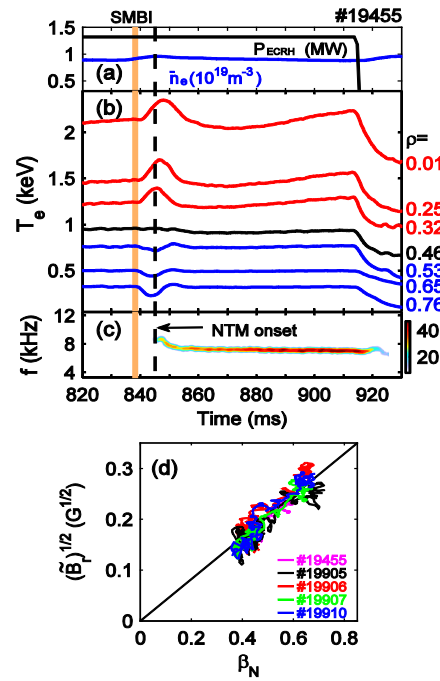


FIG. 3: Typical discharge waveforms with an onset of a 3/2 NTM during the nonlocal transport induced by SMBI in ECRH-heated plasmas at HL-2A. (a) the line-averaged density and ECRH power; (b) multi-channel ECE signals showing decrease of T_e in the plasma edge and increase of T_e in the core; (c) contour-plot of frequency spectrum of the SXR signal showing the onset of a 3/2 NTM ($f \approx 7$ kHz) during the nonlocal phase; (d) variation of the square root of \tilde{B}_r of the 3/2 island versus β_N in five discharges.

modeling [8, 10], such sheared flows should restrain the SOC or avalanche behaviors. Hence, the mechanism governing the nonlocal transport is weakened. This might explain the damping effect of an NTM island on the nonlocal transport.

In conclusion, in the HL-2A tokamak, we have investigated the properties of SOC dynamics in the nonlocal transport. Experimental evidence shows that, along with reduction of flow shear at the plasma edge, the SOC or avalanche behaviors are strongly enhanced during the prompt nonlocal phase, suggesting important role of the SOC paradigm in governing the long-distance nonlocal heat transport.

In addition, during the nonlocal experiments at HL-2A, the NTMs can be triggered by transient increase of the local pressure gradient nearby the reversion surface of the nonlocality. Meanwhile, it is found that the NTM plays a damping role on the nonlocal effects due to locally sheared flow generated at the magnetic island of the NTM.

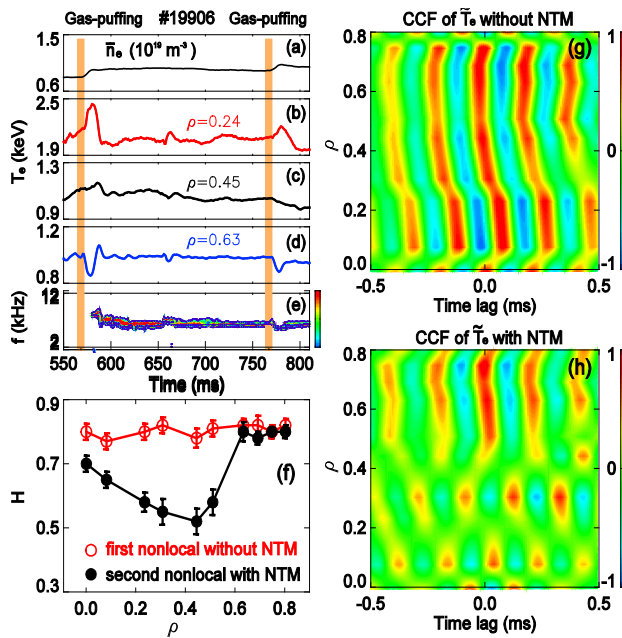


FIG. 4: Impact of NTMs on the magnitude of nonlocal transport. (a) to (e) are time evolutions of plasma density, multi-channel ECE signals and contour-plot of frequency spectrum in the SXR signal showing reduction of nonlocal effects with the presence of the 3/2 NTM; (f) radial profiles of Hurst parameters during the nonlocal phase without (red) and with (black) the NTM; (g) and (h) are contour-plot of CCF calculated in filtered ECE signals (4-7 kHz) during the nonlocality without and with the NTM, respectively.

- [1] M. W. Kissick *et al.*, Nucl. Fusion 34, 349 (1994).
- [2] K. W. Gentle *et al.*, Phys. Rev. Lett. 74, 3620 (1995).
- [3] J. D. Callen and M. W. Kissick, Plasma Phys. Controlled Fusion 39, B173 (1997).
- [4] H. J. Sun *et al.*, Plasma Phys. Controlled Fusion 52, 045003 (2010).
- [5] S. Inagaki *et al.*, Nucl. Fusion 52, 023022 (2012).
- [6] X. Ji *et al.*, IAEA Conference (St. Petersburg, Russia, 2014), EX/6-4.
- [7] T. Hwa and M. Kardar, Phys. Rev. A 45, 7002 (1992).
- [8] P. H. Diamond and T. S. Hahm, Phys. Plasmas 2, 3640 (1995).
- [9] B. A. Carreras *et al.*, Phys. Plasmas 3, 2903 (1996).
- [10] D. E. Newman *et al.*, Phys. Plasmas 3, 1858 (1996).
- [11] O. Pan *et al.*, submitted to Nucl. Fusion.
- [12] A. Davis *et al.*, J. Geophys. Res. 99, 8055 (1994).
- [13] H. E. Hurst, Trans. Am. Soc. Civ. Eng. 116, 770 (1951).
- [14] X. Ji *et al.*, to be submitted to Phys. Rev. Lett.
- [15] K. Ida *et al.*, Phys. Rev. Lett. 88, 015002 (2002).